

## High form of pentlandite and its thermal stability

ASAHIKO SUGAKI<sup>1</sup> AND ARASHI KITAKAZE<sup>2</sup>

<sup>1</sup>4-30-503, Kadan, Aoba-ku, Sendai 980, Japan

<sup>2</sup>Institute of Mineralogy, Petrology and Economic Geology, Faculty of Science, Tohoku University, Sendai 980-77, Japan

### ABSTRACT

The high-temperature form of pentlandite ( $\text{Fe}_{4.5}\text{Ni}_{4.5}\text{S}_8$ ) was found to be stable between  $584 \pm 3$  and  $865 \pm 3$  °C, breaking down into monosulfide solid solution and liquid at the later temperature. The phase is unquenchable and always displays the X-ray pattern of pentlandite (low form) at room temperature. High-temperature X-ray diffraction demonstrated that the high form has a primitive cubic cell with  $a = 5.189$  Å (620 °C) corresponding to  $a/2$  of pentlandite. The high-low inversion is reversible, accompanied by a large latent heat. It is thought to be order-disorder in character. The transition temperature falls with decreasing S content. The high form of pentlandite has a limited solid solution from  $\text{Fe}_{5.07}\text{Ni}_{3.93}\text{S}_{7.85}$  to  $\text{Fe}_{3.61}\text{Ni}_{3.39}\text{S}_{7.85}$  at 850 °C. However its solid solution extends rapidly toward  $\text{Ni}_{3 \pm x}\text{S}_2$  in the Ni-S join with decreasing temperature. High-form pentlandite with  $\text{Fe} = \text{Ni}$  in atomic percent crystallizes first by a pseudoperitectic reaction between monosulfide solid solution and liquid. The high form ( $\text{Fe} = \text{Ni}$ ) crystallized from the liquid always has the metal-rich (S-poor) composition in the solid solution at each temperature and coexists with taenite  $\gamma$  (Fe,Ni) below  $746 \pm 3$  °C. This metal-rich high-form  $\text{Fe}_{4.5}\text{Ni}_{4.5}\text{S}_{7.4}$  breaks down into pentlandite and  $\gamma$  (Fe,Ni) at  $584 \pm 3$  °C (pseudoeutectoid).

These results suggest that in geological processes, such as the formation of Ni-Cu ore deposits, pentlandite can crystallize as the high form from liquid (sulfide magma) at the comparatively high temperatures around 800 °C.

### INTRODUCTION

Kullerud (1962, 1963a) reported that pentlandite  $\text{Fe}_{4.5}\text{Ni}_{4.5}\text{S}_8$  is present as a stable phase below 610 °C, but breaks down into a mixture of  $\text{Ni}_{3 \pm x}\text{S}_2$  and pyrrhotite (monosulfide solid solution) at this temperature or above. However Sugaki et al. (1982) and Sugaki and Kitakaze (1992) found instead that pentlandite transforms into a high form at 610 °C that is stable up to 865 °C. The existence of a high-form pentlandite as the stable phase required the reexamination and revision of the Fe-Ni-S phase diagrams above 600 °C, especially in the central portion of the system, given by Kullerud (1963b), Kullerud et al. (1969), and Hsieh et al. (1982). Sugaki et al. (1984) found that high-form pentlandite shows continuous solid solution from  $\text{Fe}_{4.97}\text{Ni}_{4.03}\text{S}_{7.85}$  and  $\text{Fe}_{5.37}\text{Ni}_{3.63}\text{S}_{7.89}$  to  $\text{Ni}_{3 \pm x}\text{S}_2$  (Rosenqvist 1954; Kullerud and Yund 1962) in the Ni-S join at 800 and 650 °C, respectively.

In this paper, we present new experimental data on the thermal stability of the low form of pentlandite together with its phase transition and the phase relations of high-form pentlandite in the Fe-Ni-S system. Chemical compositions and crystal data for minerals and phases in the Fe-Ni-S ternary synthesized here are given in Table 1. Phase equilibria in the Fe-Ni-S system at temperatures from 600 to 850 °C will be reported in a subsequent paper.

### HIGH-TEMPERATURE SYNTHESSES

#### Evacuated silica glass-tube method

Fe (99.999%) and Ni (99.999%) from Johnson Matthey Co., Ltd., and S (99.99%) from Kanto Chemical Co., Ltd., were used as starting materials. The metals and S were precisely weighed in the proportion to the compositions of the pentlandite solid solution (SS), and then they were sealed in the silica tube under vacuum of  $1.33 \times 10^{-1}$  Pa ( $10^{-3}$  Torr). The sealed tubes with the charge were kept at 800 °C for 7 d after preheating at 400 to 500 °C for 3 d. The product was homogenized by grinding, resealed in an evacuated silica tube, and reheated at 650, 800, or 850 °C for at least 10 d. The tube was then cooled rapidly in ice water. The final products were aggregates of fine anhedral grains of pentlandite, 10 to 50  $\mu\text{m}$  in size. Its homogeneity was examined by reflected-light-microscopy, X-ray diffraction, and microprobe analysis, and found to be a monophase.

#### Vapor transportation method

Approximately 100 mg of powdered pentlandite ( $\text{Fe}_{4.50}\text{Ni}_{4.50}\text{S}_{7.80}$ ), synthesized as above, and 0.5 mg of iodine were sealed together in an evacuated silica tube, heated at 770 °C for 7 d in a vertical electric furnace, and then cooled to room temperature. Euhedral pentlandite corresponding to the high form had recrystallized as a fine-grained aggregate

**TABLE 1.** Chemical compositions and crystallographic data of minerals and phases in this study

Mineral names	Abbrev.	Composition	Structure type (cell edges in Å)	References
Pyrrhotite	po	Fe <sub>1-x</sub> S	Hexagonal 1C <i>a</i> = 3.45, <i>c</i> = 5.75	Nakazawa and Morimoto (1971)
Pentlandite	pn	(Fe,Ni) <sub>9</sub> S <sub>8</sub>	Cubic Fm3m <i>a</i> = 10.03	Rajamani and Prewitt (1973)
High-form pentlandite	hpn	(Fe,Ni) <sub>9</sub> S <sub>8</sub>	Cubic pc <i>a</i> = 5.189 (at 620 °C)	This study
Monosulfide solid solution	mss	(Fe,Ni) <sub>1-x</sub> S	Hexagonal <i>a</i> = 3.45, <i>c</i> = 5.6	Craig and Scott (1974)
Vaesite	vs	NiS <sub>2</sub>	Cubic Pa3 <i>a</i> = 5.670	Kerr (1945)
Godlevskite	gs	Ni <sub>7</sub> S <sub>6</sub>	Orthorhombic C222 <i>a</i> = 9.336, <i>b</i> = 11.218, <i>c</i> = 9.430	Fleet (1987)
Heazlewoodite	hz	Ni <sub>3</sub> S <sub>2</sub>	Hexagonal R32 <i>a</i> = 5.747, <i>c</i> = 7.135	Fleet (1977)
High-form heazlewoodite		Ni <sub>3-x</sub> S <sub>2</sub>	Cubic Fm3m <i>a</i> = 5.22 (at 640 °C)	Liné and Huber (1963)
Taenite	tn	γ(Fe,Ni)	Cubic Fm3m <i>a</i> = 7.146	Ramsden and Cameron (1966)
Iron	ir	αFe	Cubic <i>a</i> = 2.8664	Ramsden and Cameron (1966)

near the top of the tube. The crystal faces were principally well-developed (111) and (100) forms.

### Flux method

About 200 mg of NaCl-KCl salts with 1:1 molecular ratio and 200 mg of powdered pentlandite (Fe<sub>4.50</sub>Ni<sub>4.50</sub>S<sub>7.80</sub>) synthesized by the evacuated silica tube method were sealed in a silica glass tube under vacuum of 1.33 × 10<sup>-1</sup> Pa. The tube was kept at 800 °C for 7 d. The result was aggregates of euhedral high-form pentlandite, similar to those formed by the vapor transportation method.

## EXPERIMENTAL PROCEDURES AND RESULTS

### Microscopic examinations

Pentlandite of composition Fe<sub>4.50</sub>Ni<sub>4.50</sub>S<sub>7.80</sub> synthesized at 800 °C by the evacuated silica glass tube method is yellowish gray in color with a metallic luster at room temperature. Under the reflected light microscope, it appears light creamy white in color and has a distinct octahedral cleavage. It is isotropic. The values of its reflectance in the air are 436 nm: 38.4 ± 0.2%, 497 nm: 46.0 ± 0.2%, 546 nm: 49.1 ± 0.2%, 586 nm: 51.4 ± 0.2%, and 648 nm: 53.9 ± 0.2%. These optical properties are in accord with those found previously for pentlandite (Picot and Johan 1982; Criddle and Stanley 1986).

Fine-grained crystals of heazlewoodite, godlevskite (low form Ni<sub>7</sub>S<sub>6</sub>), and taenite γ (Fe,Ni) appeared as quench products in Ni-rich high-form pentlandite SS and (Ni,Fe)<sub>3-x</sub>S<sub>2</sub>, but high-form pentlandite samples with compositions around Ni/Fe = 1 and more than ~46 at% S were almost homogeneous after quenching.

Fine-grained euhedral crystals obtained both by vapor transportation and flux were examined by scanning electron microscope. The SEM photomicrographs of euhedral high-form pentlandite are shown in Figure 1.

### Electron probe microanalysis

Electron probe microanalysis (EPMA) was used to ascertain the homogeneity of the synthetic pentlandites and

analyze their chemical compositions. Synthetic FeS was used as a standard for Fe and S, whereas NiS was the standard for Ni. The Bence and Albee (1968) method was used for correcting the X-ray intensity ratio. Compositions of crystals grown at 800 °C in flux are in the range of Fe<sub>4.25-5.03</sub>Ni<sub>3.97-4.75</sub>S<sub>7.89-8.08</sub> (Table 2<sup>1</sup>), and generally are very close to that of the stoichiometric pentlandite.

Compositions of crystals precipitated at 770 °C by vapor transportation are in the range of Fe<sub>3.09-3.87</sub>Ni<sub>5.13-5.91</sub>S<sub>7.19-7.70</sub> (Table 3<sup>1</sup>). All the compositions correspond to those of Ni-rich high-form pentlandite SS. For the evacuated silica tube method at 850 °C, the compositions of the monophase products with Fe = Ni (in atomic percent) were Fe: 26.47, Ni: 26.47, S: 47.06 (Fe<sub>4.50</sub>Ni<sub>4.50</sub>S<sub>8.00</sub>) and (Fe<sub>4.50</sub>Ni<sub>4.50</sub>S<sub>8.00</sub>) and Fe: 26.79, Ni: 26.79, S: 46.42 (Fe<sub>4.50</sub>Ni<sub>4.50</sub>S<sub>7.80</sub>) (Table 4<sup>1</sup>). High-form pentlandite (with only monosulfide SS present or monosulfide SS and liquid present) is present as a SS of the limited range from Fe<sub>3.06</sub>Ni<sub>3.94</sub>S<sub>7.85</sub> to Fe<sub>3.61</sub>Ni<sub>5.39</sub>S<sub>7.85</sub> including Fe<sub>4.50</sub>Ni<sub>4.50</sub>S<sub>8.00</sub> (Table 5<sup>1</sup>). However the high-form pentlandite SS extends rapidly toward Ni<sub>3-x</sub>S<sub>2</sub> in the Ni-S join with decreasing temperature and reaches the join as a continuous SS below 806 °C at which point Ni<sub>3-x</sub>S<sub>2</sub> (Kullerud and Yund 1962) or Ni<sub>4</sub>S<sub>3</sub> (Lin et al. 1978) appear. From the monophase data obtained by the silica tube synthesis, we find that the high-form pentlandite SS forms a continuous SS with Ni<sub>3-x</sub>S<sub>2</sub> (or Ni<sub>4</sub>S<sub>3</sub>) at 800 and 650 °C.

### High-temperature X-ray diffraction

Because the high form of pentlandite and its SS are unquenchable, a high-temperature heating unit was used to examine one sample with composition Fe<sub>4.50</sub>Ni<sub>4.50</sub>S<sub>7.80</sub> synthesized by the evacuated silica tube method at 800 °C. Approximately 30 mg of the powdered sample was

<sup>1</sup> For a copy of Tables 2, 3, 4, 5, 7, 8, and 9, Document AM-98-001, contact the Business Office of the Mineralogical Society of America (see inside front cover of recent issue) for price information. Deposit items may also be available on the American Mineralogist web site (see inside back cover for a current web address).

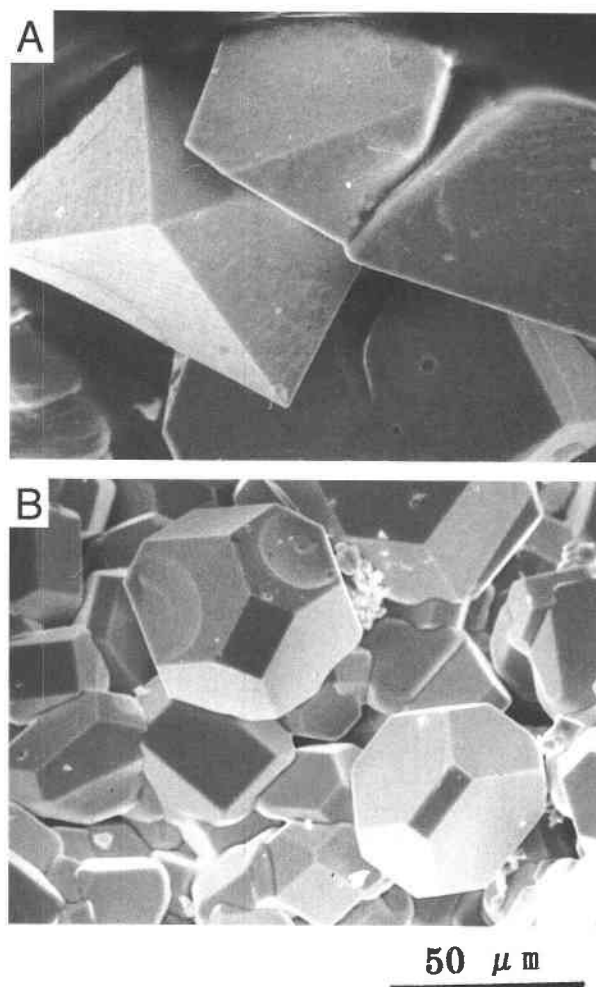


FIGURE 1. Photomicrographs of high-form pentlandite crystals by scanning electron microscope. **A** = Euhedral crystals of high-form pentlandite synthesized by the  $I_2$  vapor transportation method at 770 °C. **B** = High-form pentlandite crystals synthesized by the KCl-NaCl flux method at 800 °C.

mounted on a gold sample holder. The surface of the sample was coated with a gold film by a vacuum evaporator to keep the surface of the sample flat up to 700 °C and to prevent oxidation. The heating unit was evacuated with a rotary vacuum pump and then filled up with a purified nitrogen gas. The X-ray powder patterns for the pentlandite sample were taken using  $CuK\alpha$  (35 kV, 15 mA) from 25 to 620 °C in a slow flow of nitrogen gas. Also, the gold coating was used as a standard for correction of the reflection peaks in the powder pattern at high temperature, by using its expansion coefficient. Metallic silicon was also used as an internal standard but possibly reacted with the sample at high temperature. Temperature was measured with a Pt-Pt-Rh (13%) thermocouple inserted into a small well of the sample holder. The temperature difference between the holder well and sample was within  $\pm 2$  °C at 600 °C. The temperature during the measurement was regulated to within  $\pm 1$  °C.

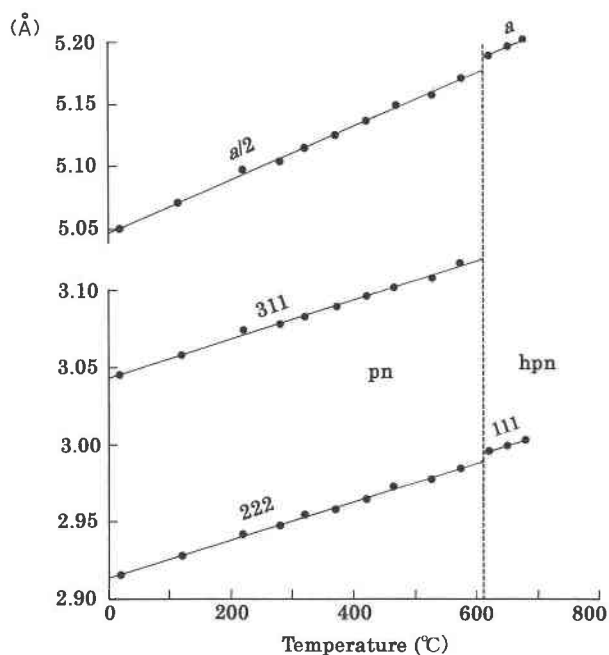


FIGURE 2. The cubic cell edges and spacings of  $d_{311}$  and  $d_{222}$  of pentlandite ( $Fe_{4.50}Ni_{4.50}S_{7.80}$ ) and  $d_{111}$  of its high form vs. the temperatures. Abbreviations: See Table 1.

Values of the cell edge and spacings  $d_{311}$  and  $d_{222}$  vs. the temperature (Fig. 2) increase linearly with increasing temperature. The linear thermal expansion coefficient of pentlandite ( $Fe_{4.50}Ni_{4.50}S_{7.80}$ ) calculated using the cell edges is  $13.4 \times 10^{-5} \text{ } ^\circ\text{C}^{-1}$  (25 to 580 °C). This value agrees very well with  $13.5 \times 10^{-5} \text{ } ^\circ\text{C}^{-1}$  (25 to 608 °C) calculated by us using the data on thermal change of the cell edge for synthetic pentlandite ( $Fe_{4.5}Ni_{4.5}S_{7.8}$ ) by Morimoto and Kullerud (1964), but larger than  $11.1 \times 10^{-5} \text{ } ^\circ\text{C}^{-1}$  (24 to 200 °C) for pentlandite from Froid, Sudbury, sample studied by Rajamani and Prewitt (1975).

The powder patterns above 620 °C differ remarkably from those of the same sample below 580 °C (Fig. 3).

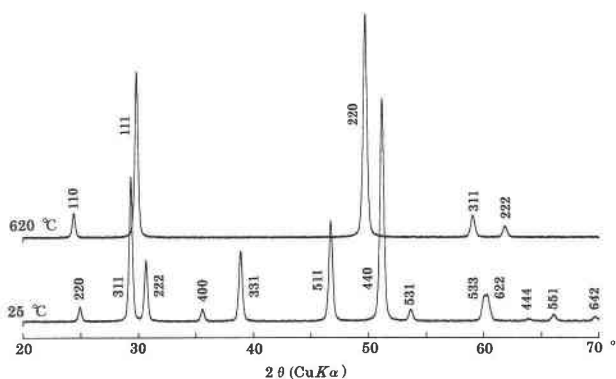


FIGURE 3. X-ray powder diffraction patterns of synthetic pentlandite and high-form pentlandite with  $Fe_{4.50}Ni_{4.50}S_{7.80}$  at 25 and 620 °C, respectively.

**TABLE 6.** X-ray powder diffraction data for synthetic pentlandite ( $\text{Fe}_{4.50}\text{Ni}_{4.50}\text{S}_{7.60}$ ) at 25, 280, and 580 °C and for high-form pentlandite at 620 °C

<i>hkl</i>	Pentlandite ( $\text{Fe}_{4.50}\text{Ni}_{4.50}\text{S}_{7.60}$ )						High-form pentlandite		
	25 °C		280 °C		580 °C		620 °C		
	<i>l</i>	<i>d</i> (obs)	<i>l</i>	<i>d</i> (obs)	<i>l</i>	<i>d</i> (obs)	<i>hkl</i>	<i>l</i>	<i>d</i> (obs)
111	24	5.84	20	5.89	25	5.97			
200	6	5.051	5	5.104	5	5.172			
220	6	3.571	5	3.607	5	3.656	110	10	3.649
311	60	3.045	40	3.077	45	3.119			
222	25	2.916	15	2.945	20	2.988	111	70	2.996
400	5	2.524	2	2.551	2	2.584			
331	30	2.317	15	2.342	10	2.374			
511	44	1.945	30	1.966	25	1.990			
440	100	1.786	100	1.804	100	1.825	220	100	1.835
531	5	1.708	2	1.728	2	1.749			
533	10	1.541	5	1.557	5	1.577			
622	9	1.533	7	1.538	7	1.558	311	10	1.564
444	1	1.457	2	1.473	2	1.493	222	5	1.500
551	3	1.414	2	1.429	2	1.449			
642	2	1.349	2	1.364	1	1.382			
<i>a</i>		10.100(1)		10.206(2)		10.344(2)			5.189(3) Å

Note: Radiation =  $\text{CuK}\alpha$  (35 kV, 15 mA). Scanning speed of goniometer = 1°/min.

The reflections of type  $hkl \neq 2n$  below 580 °C disappear at 620 °C, but reflections of type  $hkl = 2n$  remain. Because all the reflections at 620 °C correspond to those of the even number indices of pentlandite below 580 °C, they were indexed in terms of a cubic cell with  $a/2$  of pentlandite below 580 °C (Table 6). The change is reversible. At 620 °C, reflections that indicate the appearance of other phases, for instance monosulfide SS, were not found.

X-ray diffraction data for single crystals of high-form pentlandite synthesized by both the vapor transportation and flux methods at 770 and 800 °C, respectively, were obtained using a precession camera with a platinum wire furnace. A single crystal of pentlandite was placed inside a 0.5 mm diameter silica glass capillary and fixed with a silica glass fiber inserted into the tube. The capillary was evacuated and sealed. The sample was equilibrated at the desired temperature for one day, then an exposure was taken over 2 d. Temperature was measured with a chromel-alumel thermocouple set 3 mm from the specimen tube and controlled continuously within  $\pm 1$  °C by a regulator. The temperature difference between specimen and the head of the thermocouple was within  $\pm 5$  °C at 600 °C.

A representative [110] precession photograph of synthetic pentlandite ( $\text{Fe}_{4.56}\text{Ni}_{4.44}\text{S}_{7.95}$ ) at room temperature (25 °C) is shown in Figure 4A. Diffraction patterns taken at 200, 400, and 580 °C are similar. However the precession photograph at 620 °C (Fig. 4B), differs markedly. Reflections of the odd number indices seen in the photographs below 580 °C disappear at 620 °C, but those of the even number indices remain at high temperature. These reflections at 620 °C are indexed as 110, 111, and 220 for the cubic cell with a cell edge that is half of the low form of pentlandite as seen in the photograph. The cubic cell edge of the single crystal at 620 °C is  $a = 5.19$  Å. This value

of the cell edge is in good agreement with that obtained from the powder data at 620 °C. The diffraction pattern for the single crystal, cooled down to room temperature from 620 °C, returned to the original form (Fig. 4A).

Similar results were obtained for the high-temperature powder and single-crystal patterns of natural pentlandite ( $\text{Fe}_{4.11}\text{Ni}_{4.85}\text{Co}_{0.08}\text{S}_{7.96}$ ) from Copper Cliff, Sudbury.

It is clear that a reversible phase transition occurs at a temperature between 580 and 620 °C in which the size of unit-cell edge doubles. No compositional change at the transition is found, and it is possible that this transition is an order-disorder inversion from the supercell (low form) to the subcell.

#### Differential thermal analysis

To ascertain the thermal behavior and stability of pentlandite, differential thermal analysis (DTA) was performed using an evacuated silica glass tube as a reaction vessel. A sample synthesized at 800 °C by the evacuated silica tube method was used. Alpha alumina was used as a reference material. Chromel-alumel thermocouples were used for both the differential and sample temperatures.

DTA was normally carried out at fixed heating rates of 5 and 10 °C/min from room temperature to 1000 °C or above. Sometimes the DTA was performed at a slower heating rate of 1 and 2 °C/min from 550 to 1000 °C to pinpoint the temperatures of the thermal reactions more accurately. The sample heated up to above 1000 °C was also cooled in the furnace, and the DTA curve on the cooling was obtained again at the spontaneous cooling rate of the furnace. Temperatures were calibrated using the melting points of high-purity tin (231.97 °C), zinc (419.6 °C), aluminum (660.4 °C), and silver (961.9 °C).

Two strong endothermic reactions beginning at 610 and 865 °C are seen during heating (Fig. 5, curve A). The

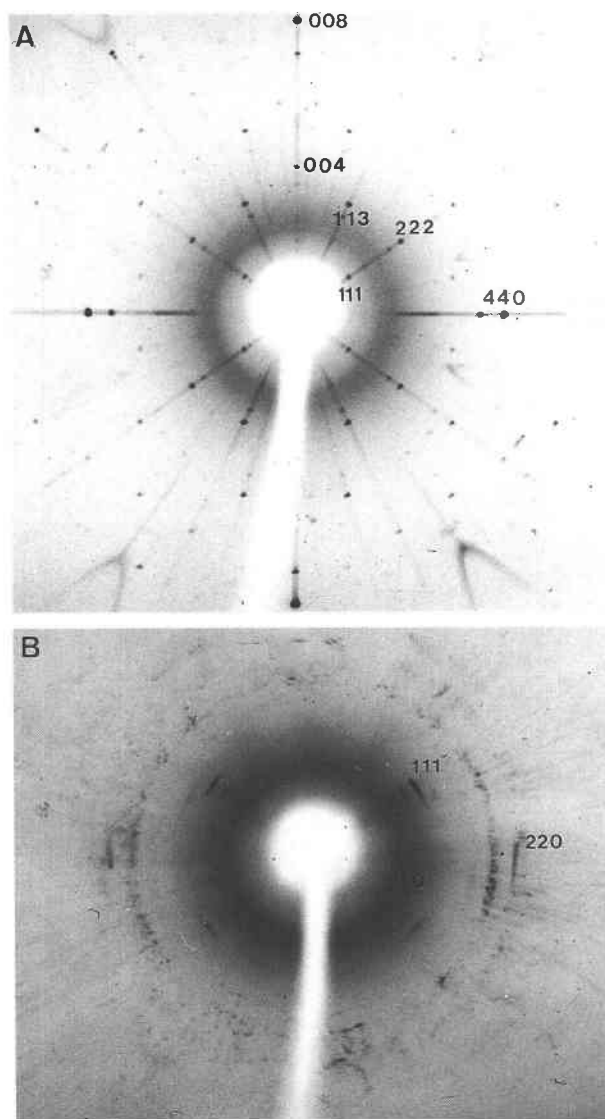


FIGURE 4. Two [110] precession photographs for a single crystal of synthetic low- and high-form pentlandites with  $\text{Fe}_{4.50}\text{Ni}_{4.44}\text{S}_{7.95}$  at 25 and 620 °C, respectively. A = 25 °C; B = 620 °C.

later reaction still continues with increasing temperature and finishes at 952 °C. These reactions also appear as the exothermic peaks during cooling (curve B). The continuous reaction from 865 to 952 °C in the heating curve (Fig. 5A) is clearly seen in the cooling curve (Fig. 5B).

From microscope observations, EPMA, X-ray diffraction, and DTA, we conclude that the feature at 610 °C is due to a high-low inversion, and the feature at 865 °C arises from the breakdown of high-form pentlandite into monosulfide SS and liquid. The continuous reaction between 865 and 952 °C corresponds to successive melting of monosulfide SS, which is a breakdown product of high-form pentlandite at 865 °C. Finally the remnant monosulfide SS melts at  $952 \pm 5$  °C.

The transition temperature of pentlandite with Fe = Ni

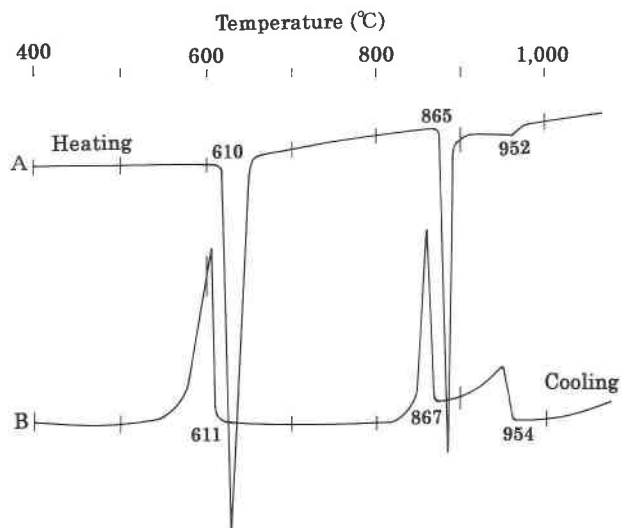


FIGURE 5. DTA Curves of synthetic pentlandite (and high-form pentlandite) with  $\text{Fe}_{4.50}\text{Ni}_{4.50}\text{S}_{7.80}$ . (A) Heating curve of 10 °C/min. (B) Cooling curve.

(in at%) at around 600 °C depends on composition, especially S content. The transition temperature of  $\text{Fe}_{4.50}\text{Ni}_{4.50}\text{S}_{7.90}$  with monosulfide SS is  $615 \pm 3$  °C, a slightly higher temperature than that of  $\text{Fe}_{4.50}\text{Ni}_{4.50}\text{S}_{7.80}$ . However the transition of metal-rich (S-poor) pentlandite ( $\text{Fe}_{4.50}\text{Ni}_{4.50}\text{S}_{7.70}$ ) occurs over a temperature range from 586 to 604 °C, as is discussed below.

## HIGH-FORM PENTLANDITE PHASE RELATIONS

### Isothermal phase relations at 850 °C

Phase relations of high-form pentlandite in the metal-rich portion of the Fe-Ni-S system (Fig. 6) were determined from optical properties, X-ray powder diffraction data, and EPMA (Table 8'). High-form pentlandite appears as a stable phase at 850 °C with a limited SS from  $\text{Fe}_{5.07}\text{Ni}_{3.93}\text{S}_{7.85}$  to  $\text{Fe}_{3.61}\text{Ni}_{5.39}\text{S}_{7.85}$  including stoichiometric  $\text{Fe}_{4.50}\text{Ni}_{4.50}\text{S}_{8.00}$  and coexists with monosulfide SS in the S-rich side and liquid in the metal-rich side. High-form pentlandite samples of both the Fe- and Ni-rich ends of the SS coexist with each monosulfide SS and liquid as univariant assemblages. However high-form pentlandite cannot coexist with taenite  $\gamma$  (Fe,Ni) at 850 °C because of existence of the extensive liquid field.

### Thermal stabilities of pentlandites

A phase diagram of the S compositions from 35 to 52 at% with Fe = Ni vs. the temperatures was constructed (Fig. 7) using the equilibrium experiment data (Table 9') and the DTA data (Table 10). Both high- and low-form samples with Fe = Ni show limited SS across a restricted S-composition range. A small two-phase field containing both forms of pentlandite is found between 584 and 615 °C. Pentlandite of composition  $\text{Fe}_{4.50}\text{Ni}_{4.50}\text{S}_{7.90}$  coexists with monosulfide SS and inverts to high-form pentlandite at  $615 \pm 3$  °C. However the transition temperature falls

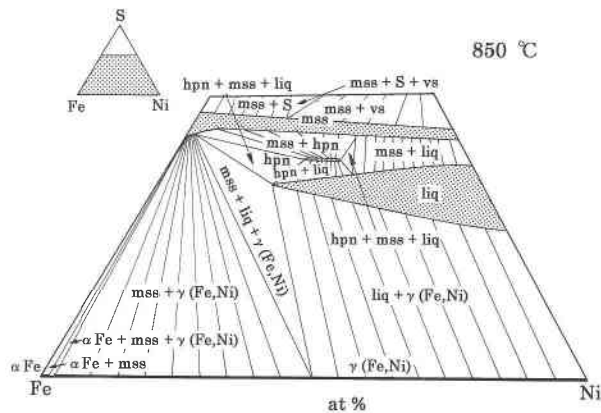


FIGURE 6. The phase relations of the metal-rich portion in the Fe-Ni-S system at 850 °C. Abbreviations: See Table 1; liq = liquid.

from 615 to 584 °C with decreasing the S content. This transition is reversible.

High-form pentlandite of a metal-rich composition generally shows fine-grained crystals of  $\gamma$  (Fe,Ni) when quenched. In these circumstances, we were able to distinguish the high-form pentlandite from the low form under the microscope and by EPMA. However, as seen in S-rich high-form pentlandite, when  $\gamma$  (Fe,Ni) did not appear by quenching, it proved difficult to distinguish both the two phases after quench.

High-form pentlandite ( $\text{Fe}_{4.50}\text{Ni}_{4.50}\text{S}_{7.90}$ ) is stable up to  $865 \pm 3$  °C, when it breaks down into monosulfide SS and liquid. The products of the breakdown of high-form pentlandite of composition  $\text{Fe}_{4.50}\text{Ni}_{4.50}\text{S}_{7.80}$  (Fe = Ni: 26.79 at% and S: 46.42 at%) at 880 °C are shown in Figure 8 (and Table 9<sup>1</sup>). At 1000 °C, the entire charge is similar in appearance to the liquid patch shown in Figure 8. A pseudo-eutectic point exists at  $746 \pm 3$  °C and 39.3 at% S in the metal-rich portion of the binary. The most metal-rich high-form pentlandite SS (Fe = Ni) coexisting with  $\gamma$  (Fe,Ni) breaks down into pentlandite (low form) and  $\gamma$  (Fe,Ni) in the pseudo-eutectoid reaction at  $584 \pm 3$  °C and 45.2 at% S (Fig. 7).

## DISCUSSION

As mentioned above, the thermal stability range of pentlandite including its high form in fact extends up to 865 °C, approximately 255 °C higher than 610 °C suggested by Kullerud (1962, 1963a). The phase diagram of the Fe-Ni-S system at temperatures above 600 °C by Kullerud (1963b), Kullerud et al. (1969), and Hsieh et al. (1982) should now be re-appraised because the high form of pentlandite was not previously identified, although they did report a ternary phase  $(\text{Ni,Fe})_{3\pm x}\text{S}_2$  near the Ni-S join at 860 (Kullerud 1963b) and 850 °C (Hsieh et al. 1982). The high form of pentlandite has a SS with a limited range from  $\text{Fe}_{5.07}\text{Ni}_{3.93}\text{S}_{7.85}$  to  $\text{Fe}_{3.61}\text{Ni}_{5.39}\text{S}_{7.85}$  including  $\text{Fe}_{4.50}\text{Ni}_{4.50}\text{S}_{8.00}$  at 850 °C (Fig. 6).

We have found that the high-form pentlandite SS extends

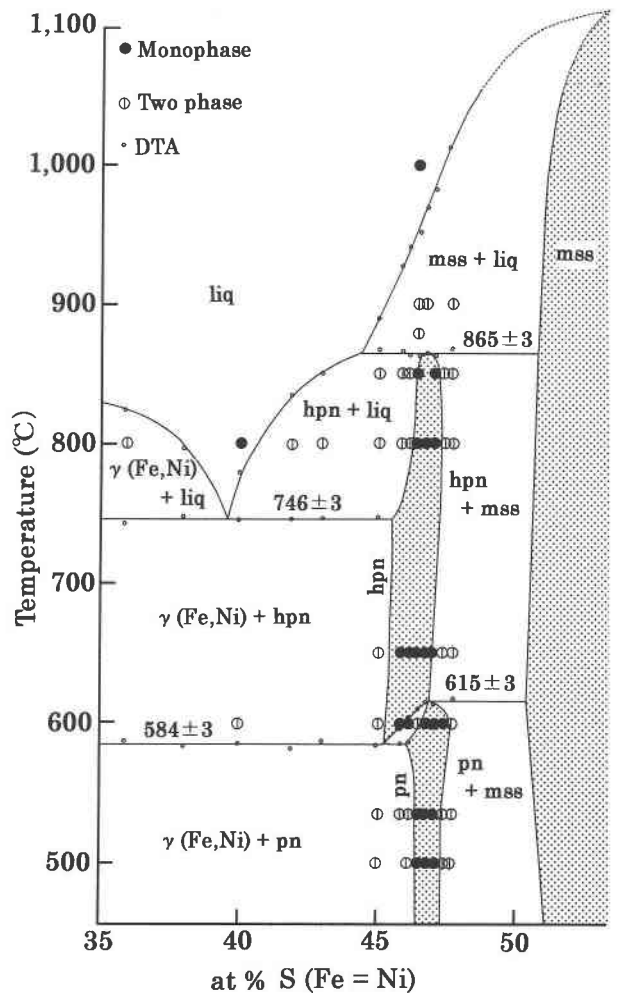


FIGURE 7. The phase diagram of the sulfur composition with Fe = Ni vs. the temperature. The boundary of monosulfide SS below 600 °C referred to Naldrett et al. (1967). Abbreviations: See Table 1; liq = liquid

rapidly to the Ni-rich direction with decreasing temperature, and continues with  $\text{Ni}_{3\pm x}\text{S}_2$  below 806 °C, the breakdown (or incongruent melting) temperature of  $\text{Ni}_{3\pm x}\text{S}_2$  (Kullerud and Yund 1962). The compositional data of high-form pentlandite SS and  $(\text{Fe,Ni})_{3\pm x}\text{S}_2$  synthesized at 800 °C indicate the existence of a continuous SS between high-form pentlandite and  $\text{Ni}_{3\pm x}\text{S}_2$ . The SS is maintained at 650 °C. These results are in agreement with other recent findings: Fedorova and Sinyakova (1993) found high-form pentlandite SS (heazlewoodite SS in their terminology) at 820 °C. Karup-Møller and Makovicky (1995) also reported the existence of a continuously extensive SS,  $(\text{Fe,Ni})_{3\pm x}\text{S}_2$ , between high-form pentlandite and  $\text{Ni}_{3\pm x}\text{S}_2$  at 725 °C.

The crystallization of the high form of pentlandite with Fe = Ni may now be understood from Figure 7 as follows: The high form crystallizes first by a pseudoperitectic reaction between monosulfide SS and liquid at  $865 \pm 3$  °C and successively precipitates directly from the liquid

**TABLE 10.** Temperatures of the phase reactions obtained by DTA in the composition range from 35 to 48 at% S of the (Fe<sub>0.5</sub>Ni<sub>0.5</sub>)-S join in the Fe-Ni-S system

Run no.	at%			°C				
	Fe	Ni	S	T <sub>1</sub>	T <sub>2</sub>	T <sub>3</sub>	T <sub>4</sub>	T <sub>5</sub>
FNS3876	26.16	26.16	47.68		618		868	1012
FNS3871	26.47	26.47	47.06		613		863	982
FNS4002	26.63	26.63	46.74		615		865	970
FNS3869	26.79	26.79	46.42		600-610		865	952
FNS4001	26.95	26.95	46.10		586-604		864	941
FNS3873	27.11	27.11	45.78	584	595		866	928
FNS3936	27.50	27.50	45.00	583		747	868	890
FNS3937	28.50	28.50	43.00	587		747		851
FNS3960	29.03	29.03	41.94	581		746		835
FNS3980	30.00	30.00	40.00	585		745		780
FNS3959	31.03	31.03	37.94	584		749		797
FNS3958	32.14	32.14	35.72	587		743		825
				584 ± 3		746 ± 3		865 ± 3

Note: T<sub>1</sub> = Pseudoeutectoid; T<sub>2</sub> = Inversion between pentlandite and high-form pentlandite; T<sub>3</sub> = Pseudoeutectic; T<sub>4</sub> = Breakdown (incongruent melting) of high-form pentlandite; T<sub>5</sub> = Liquidus (completely melting).

with decreasing temperature down to  $746 \pm 3$  °C, corresponding to a pseudoeutectic in the ternary. This pseudoeutectic continues to a eutectic point at 637 °C and 33 at% S in the Ni-S join (Singleton et al. 1991). The high-form pentlandite crystallized from liquid below 865 °C has the metal-rich composition at each temperature and always coexists with  $\gamma$  (Fe,Ni) below 746 °C in the equilibrium state. This metal-rich high-form pentlandite (Fe<sub>4.5</sub>Ni<sub>4.5</sub>S<sub>7.4</sub>) breaks down into pentlandite (low form) and  $\gamma$  (Fe,Ni) as a pseudoeutectoid reaction at  $584 \pm 3$  °C and 45.2 at% S. The pseudoeutectoid continues to a ternary eutectoid point at 470 °C and approximately 13 Fe, 49 Ni, and 38 S in atomic percentages near the Ni-S boundary in the Fe-Ni-S system (Fedorova and Sinyakova 1993). On the other hand, high-form pentlandite (Fe<sub>4.50</sub>Ni<sub>4.50</sub>S<sub>7.90</sub>) coexisting with monosulfide SS inverts into pentlandite of the same composition at  $615 \pm 3$  °C.

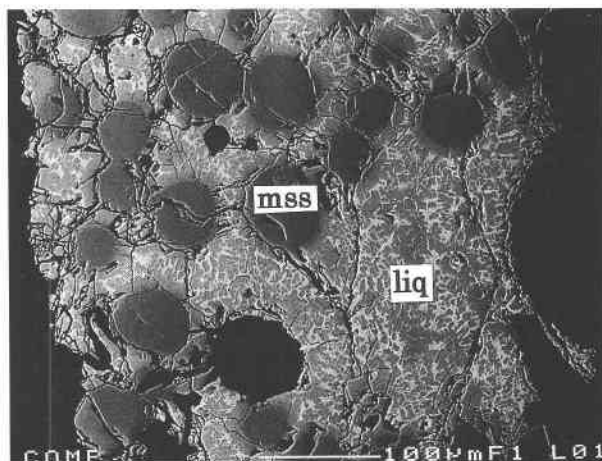


**FIGURE 8.** Back-scattered electron images by EPMA for the breakdown products of high-form pentlandite (Fe<sub>4.50</sub>Ni<sub>4.50</sub>S<sub>7.80</sub>) at 880 °C into monosulfide SS and liquid (liq), which is a mixture of pentlandite (dark gray) and  $\gamma$  (Fe,Ni) (light gray) as quenched products. Abbreviations: See Table 1.

This inversion temperature falls continuously from 615 to  $584 \pm 3$  °C with decreasing S content. Because the inversion passes through a two-phase field of coexisting high- and low-form pentlandites within the loop, the inversion should exist over some temperature range (maximum 20 °C in Fig. 7). However this temperature range was difficult to detect precisely by DTA.

The existence of high-form pentlandite as a stable phase up to 865 °C (the breakdown temperature of high-form pentlandite) shows that the previous inference of pentlandite genesis by Kullerud (1962, 1963a) are probably incorrect. High-form pentlandite with Fe = Ni can crystallize from liquid at temperatures between 865 and 746 °C (Fig. 7). The existence of a stable high-form pentlandite phase at high temperature is supported by the observation of genesis of Ni-Cu ores with pentlandite crystallized directly from sulfide magma (Lindgren 1933; Bateman 1952).

When pentlandite inverts into high-form pentlandite, a large latent heat anomaly is displayed in the DTA curve (Fig. 5). The enthalpy appears to be as much as or nearly equal to that of the latent heats of melting and breakdown reactions. Kullerud (1962), therefore, believed that the strong peak at 610 °C could not be explained as the result of a polymorphic inversion but rather indicates the breakdown of the pentlandite phase. Our experiments, however, refute this interpretation. Such a large latent heat of inversion is a rare case in sulfide and is thought to be caused by a peculiarity of the pentlandite crystal structure, which is characterized by alternating the arrangement of subcells with eight tetrahedrally coordinated cations and with an octahedrally coordinated cation (Lindqvist et al. 1936; Rajamani and Prewitt 1973). Apparently, transformation of such a distinctively ordered structure into a disordered primitive cubic cell can cause a large heat anomaly.

#### ACKNOWLEDGMENTS

The authors are grateful for assistance by T. Hayashi in the experiments. We thank Simon A.T. Redfern for his helpful suggestions and reviews of the manuscript, and two anonymous reviewers for their critical comments.

## REFERENCES CITED

- Bateman, A.M. (1952) *Economic mineral deposits*, 875 p. Wiley, London.
- Bence, A.E. and Albee, A.L. (1968) Empirical correction factors for the electron microanalysis of silicate and oxides. *Journal of Geology*, 76, 382–403.
- Craig, J.R. and Scott, S.D. (1974) Sulfide phase equilibria. *Mineralogical Society of America Short Course Notes*, CS1–110.
- Criddle, A.J. and Stanley, C.J. (1986) The quantitative data file for ore minerals. The Commission on Ore Microscopy of the International Mineralogical Association, 275 p. British Museum, London.
- Fedorova, Z.N. and Sinyakova, E.F. (1993) Experimental investigation of physicochemical conditions of pentlandite formation. *Geologiya i Geofizika*, 34, 84–92 (in Russian).
- Fleet, M.E. (1977) The crystal structure of heazlewoodite and metallic bonds in sulfide minerals. *American Mineralogist*, 62, 341–345.
- (1987) Structure of godlevskite,  $\text{Ni}_3\text{S}_8$ . *Acta crystallographica*, C43, 2255–2257.
- Hsieh, K.-C., Chang, Y.A., and Zhong, T. (1982) The Fe-Ni-S system above 700 °C. *Bulletin of Alloy Phase Diagrams*, 3, 165–172.
- Karup-Møller, S. and Makovicky, E. (1995) The phase system Fe-Ni-S at 725 °C. *Neues Jahrbuch für Mineralogie Monatshefte*, 1–10.
- Kerr, P.F. (1945) Cattierite and vaesite: New Co-Ni minerals from the Belgian Congo. *American Mineralogist*, 30, 483–497.
- Kullerud, G. (1962) The Fe-Ni-S system. *Carnegie Institute of Washington Year Book*, 61, 144–150.
- (1963a) Thermal stability of pentlandite. *Canadian Mineralogist*, 7, 353–366.
- (1963b) The Fe-Ni-S system. *Carnegie Institute of Washington Year Book*, 62, 175–189.
- Kullerud, G. and Yund, R.A. (1962) The Ni-S system and related minerals. *Journal of Petrology*, 3, 126–175.
- Kullerud, G., Yund, R.A., and Moh, G.H. (1969) Phase relations in the Cu-Fe-S, Cu-Ni-S, and Fe-Ni-S systems. In H.D.B. Wilson, Ed., *Magmatic ore deposits*, p. 323–343. *Economic Geology Monograph* 4.
- Lin, R.Y., Hu, D.C., and Change, Y.A. (1978) Thermodynamics and phase relationships of transition metal-sulfur system: II. The nickel-sulfur system. *Metallurgical Transactions B*, 9B, 531–538.
- Lindgren, W. (1933) *Mineral deposits* (4th edition), 930 p. McGraw-Hill Book Co., New York.
- Lindqvist, M., Lundqvist, D., and Westgren, A. (1936) The crystal structure of  $\text{Co}_9\text{S}_8$  and of pentlandite  $(\text{Ni,Fe})_9\text{S}_8$ . *Kemisk Tidskrift*, 48, 156–160.
- Liné, G. and Huber, M. (1963) Étude radiocristallographique à haute température de la phase non stoechiométrique  $\text{Ni}_{1-x}\text{S}_2$ . *Comptes Rendus de l'Académie des Sciences*, 256, 3118–3120.
- Morimoto, N. and Kullerud, G. (1964) Pentlandite thermal expansion. *Carnegie Institute of Washington Year Book*, 63, 204–205.
- Nakazawa, H. and Morimoto, N. (1971) Phase relations and super-structures of pyrrhotite,  $\text{Fe}_{1-x}\text{S}$ . *Material Research Bulletin*, 6, 345–358.
- Naldrett, A.J., Craig, J.R., and Kullerud, G. (1967) The central portion of the Fe-Ni-S system and its bearing on pentlandite exsolution in iron-nickel sulfide ores. *Economic Geology*, 62, 826–847.
- Picot, P. and Johan, Z. (1982) *Atlas of ore minerals*, p. 293–294. Elsevier, Amsterdam.
- Rajamani, V. and Prewitt, C.T. (1973) Crystal chemistry of natural pentlandites. *Canadian Mineralogist*, 12, 178–187.
- Rajamani, V. and Prewitt, C.T. (1975) Thermal expansion of the pentlandite structure. *American Mineralogist*, 60, 39–48.
- Ramsden, A.R. and Cameron, E.N. (1966) Kamacite and taenite super-structures and a metastable tetragonal phase in iron meteorites. *American Mineralogist*, 51, 37–55.
- Rosenqvist, T. (1954) A thermodynamic study of the iron, cobalt, and nickel sulfides. *Journal of the Iron and Steel Institute*, 176, 37–57.
- Singleton, S., Nash, P., and Lee, K.J. (1991) Ni-S. In T.B. Massalski, J.L. Munay, L.H. Bennet, and H. Baker, Eds., *Binary alloy phase diagram*, vol. 1, p. 2850–2853. American Society for Metals, Metal Park, Ohio.
- Sugaki, A. and Kitakaze, A. (1992) Phase transition of pentlandite. Abstracts, 29th International Geological Congress, vol. 3, 676 p. Kyoto, Japan.
- Sugaki, A., Kitakaze, A., and Hayashi, T. (1982) High-temperature phase of pentlandite. Abstracts, Annual Meeting of the Mineralogical Society of Japan, 22 p. (in Japanese).
- (1984) The solid solution of pentlandite and its phase relations at temperatures from 600 to 800 °C (abst.). *Journal of the Japanese Association of Mineralogists, Petrologists and Economic Geologists*, 79, 175–176 (in Japanese).

MANUSCRIPT RECEIVED JULY 8, 1996

MANUSCRIPT ACCEPTED AUGUST 25, 1997